QUANTIFYING DEFORMATION USING INFORMATION THEORY: THE LOG-UNBIASED NONLINEAR REGISTRATION

Igor Yanovsky[1], *Ming-Chang Chiang*[2], *Paul M. Thompson*[2], *Andrea D. Klunder*[2], *James T. Becker*[3], *Simon W. Davis*[3], *Arthur W. Toga*[2], *and Alex D. Leow*[2,4]

[1]Department of Mathematics, UCLA, Los Angeles, CA, USA
[2]Laboratory of Neuro Imaging, UCLA David Geffen School of Medicine, Los Angeles, CA, USA
[3]University of Pittsburgh Medical Center, Pittsburgh, PA, USA
[4]Neuropsychiatric Institute, UCLA David Geffen School of Medicine, Los Angeles, CA, USA

ABSTRACT

In the past decade, information theory has been studied extensively in medical imaging. In particular, maximization of mutual information has been shown to yield good results in multi-modal image registration. In this paper, we apply information theory to quantifying the magnitude of deformations. We examine the statistical distributions of Jacobian maps in the logarithmic space, and develop a new framework for constructing image registration methods. The proposed framework yields both theoretically and intuitively correct deformation maps, and is compatible with large-deformation models. In the results section, we tested the proposed method using a pair of serial MRI images. We compared our results to those computed using the viscous fluid registration method, and demonstrated that the proposed method is advantageous when recovering voxel-wise local tissue change.

Index Terms – Image registration, information theory, biomedical imaging.

1. INTRODUCTION AND THEORY

Nonlinear image registration is a well-established field in medical imaging with many applications in functional and anatomic brain mapping, image-guided surgery, and multimodality image fusion [1, 2, 3]. The goal of image registration is to align, or spatially normalize, one image to another. In multi-subject studies, this serves to reduce subject-specific anatomic differences by deforming individual images onto a population average brain template.

In this paper, we study smooth deformations $\vec{h}$ that map computational domain Ω bijectively onto itself. Let us assume, without loss of generality, that the volume of this domain is 1, i.e., $|\Omega| = 1$. The inverse map of $\vec{h}$ is denoted as $\vec{h}^{-1}$ and the Jacobian matrix of $\vec{h}$ as $D\vec{h}$. The Jacobian map can thus be defined as the determinant of the Jacobian matrix $|D\vec{h}|$.

In volumetric studies, the determinant of the Jacobian matrix (density) applied to any deformation $\vec{h}$ is an important quantity, encoding the voxelwise volume change. As $\vec{h}$ (and $\vec{h}^{-1}$) is bijective and thus globally volume preserving, we have the following preservation of global density: $\int_\Omega |D\vec{h}(\xi)|d\xi = 1$, $\int_\Omega |D\vec{h}^{-1}(\xi)|d\xi = 1$. Given global preservation of density maps, we can associate three probability density functions to $\vec{h}$, $\vec{h}^{-1}$, and the identity map (id): $P_h(\cdot) = |D\vec{h}(\cdot)|$, $P_{h^{-1}}(\cdot) = |D\vec{h}^{-1}(\cdot)|$, $P_{id}(\cdot) = 1$. Differentiating the identity $\vec{h}^{-1}(\vec{h}(\vec{x})) = \vec{x}$ on both sides and setting $\vec{y} = \vec{h}(\vec{x})$, we obtain $D\vec{h}^{-1}(\vec{y}) \cdot D\vec{h}(\vec{x}) = id$, and hence, $|D\vec{h}^{-1}(\vec{y})| \cdot |D\vec{h}(\vec{x})| = 1$.

By identifying deformations with their corresponding global density maps, we can now apply information theory to quantifying the magnitude of deformations. In our approach, we choose the symmetric Kullback-Leibler (sKL) distance: $sKL = KL(P_{id}, P_h) + KL(P_h, P_{id})$ to measure the magnitude of any deformation $\vec{h}$. Here KL, the Kullback-Leibler distance between two probability density functions X and Y, is defined as $KL(X, Y) = \int_\Omega X \log X/Y dx \geq 0$. To motivate this approach, notice that the first part of sKL measure is simply integrating the log-density over the entire computational image domain:

$$\begin{aligned}\int_\Omega \log |D\vec{h}(\vec{x})|d\vec{x} &= -\int_\Omega \log \frac{1}{|D\vec{h}(\vec{x})|}d\vec{x} \\ &= -\int_\Omega P_{id} \log \frac{P_{id}}{P_h}d\vec{x} \\ &= -KL(P_{id}, P_h) \leq 0.\end{aligned} \tag{1}$$

To attach geometric meaning to the second term, we notice that the KL distance has skew-symmetry with respect to $\vec{h}$ and its inverse

$$\begin{aligned}KL(P_{id}, P_{h^{-1}}) &= -\int_\Omega \log |D\vec{h}^{-1}(\vec{y})|d\vec{y} \\ &= \int_\Omega \big(\log |D\vec{h}(\vec{x})|\big)|D\vec{h}(\vec{x})|d\vec{x} \\ &= \int_\Omega P_h \log \frac{P_h}{P_{id}}d\vec{x} \\ &= KL(P_h, P_{id}),\end{aligned} \tag{2}$$

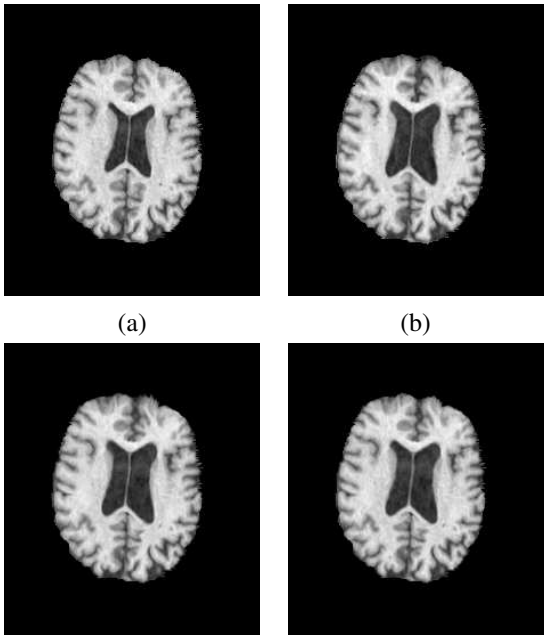

(a) (b) (c) (d)

Fig. 1. Serial MRI example. (a) image T; (b) image S; (c) image T is deformed to image S using Christensen's model; (d) image T is deformed to image S using the proposed model.

where the second equality was obtained using a change of variables, $\vec{y} = \vec{h}(\vec{x})$. Similarly, we have $KL(P_{id}, P_h) = KL(P_{h^{-1}}, P_{id})$. As a result, the following equivalent forms hold for the proposed measure

$$\begin{aligned} sKL(P_h, P_{id}) &= KL(P_h, P_{id}) + KL(P_{h^{-1}}, P_{id}) \\ &= KL(P_h, P_{id}) + KL(P_{id}, P_h) \\ &= KL(P_{id}, P_{h^{-1}}) + KL(P_{id}, P_h) \\ &= KL(P_{id}, P_{h^{-1}}) + KL(P_{h^{-1}}, P_{id}) \\ &= \int_\Omega \big(|D\vec{h}(\vec{x})| - 1\big) \log |D\vec{h}(\vec{x})| d\vec{x} \\ &= \int_\Omega \big(|D\vec{h}^{-1}(\vec{y})| - 1\big) \log |D\vec{h}^{-1}(\vec{y})| d\vec{y}. \end{aligned} \tag{3}$$

Notice that the values of non-symmetric KL distance might be negative at certain voxels. For symmetric KL distance, this does not happen. Moreover, for self-crossing maps, the symmetric KL distance (3) is undefined ($-\infty$) and thus such maps are never obtained as a result of energy minimization. Lastly, as we will show in the results section, this approach will also lead to both theoretically and intuitively correct Jacobian maps.

2. IMPLEMENTATION

Let us denote the template image as $T(\vec{x})$ and the study image as $S(\vec{x})$ defined on the spatial domain Ω. We solve for deformation $\vec{h}$, such that $T \circ \vec{h}$ matches S, while minimizing the symmetric KL distance in equation (3). The deformation $\vec{h}$ is

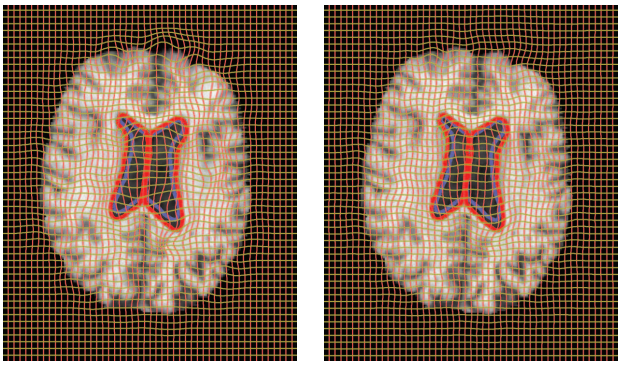

(a) (b)

Fig. 2. Serial MRI example. Results obtained with (a) Christensen's model and (b) the proposed model. Blue, yellow and red contours represent the boundaries of ventricles in T, S, and deformed T, respectively. Note that for both methods, yellow contour is essentially invisible due to a very close match. However, the resulting grid of the proposed method is visually more regular.

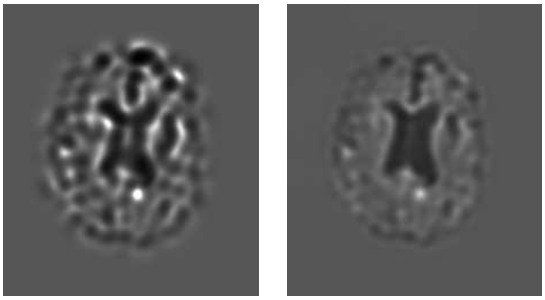

(a) (b)

Fig. 3. Serial MRI example. Jacobian map of the deformation using (a) Christensen's model and (b) the proposed model.

usually expressed at each voxel in terms of the displacement vector $\vec{u}$ from the original position: $\vec{h}(\vec{x}) = \vec{x} - \vec{u}(\vec{x})$. In this paper, we will use the sum of the squared differences (SSD) to measure the accuracy of matching between the deformed template and the study: $SSD(T, S, \vec{u}) = \frac{1}{2}\int_\Omega |T(\vec{x} - \vec{u}) - S(\vec{x})|^2 \, d\vec{x}$, which is also known as a Gaussian sensor model. To numerically implement our approach, we propose to minimize a combined cost function $C = SSD + \lambda(sKL)$. This can be achieved using incremental updating along the gradient descent of the corresponding Euler-Lagrange equation. Hence, we obtain the ith component of the force field:

$$\begin{aligned} f_i(\vec{x}, \vec{u}(\vec{x}, t)) &= -[T(\vec{x} - \vec{u}) - S(\vec{x})] \left.\frac{\partial T}{\partial x_i}\right|_{\vec{x}-\vec{u}} \\ -\lambda \sum_j \frac{\partial}{\partial x_j} \Bigg[\Big(1 + \log |D\vec{h}(\vec{x})| - &\frac{1}{|D\vec{h}(\vec{x})|}\Big) Co_{ij}(\vec{x}) \Bigg], \\ \big(D\vec{h}(\vec{x})\big)^{-1} &= \frac{\big(Co_{ij}(\vec{x})\big)^T}{|D\vec{h}(\vec{x})|}, \end{aligned} \tag{4}$$

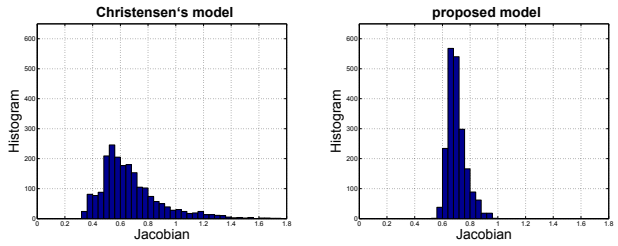

Fig. 4. Serial MRI example. Histograms of Jacobian values of the deformations inside the ventricle for Christensen's model and the proposed model.

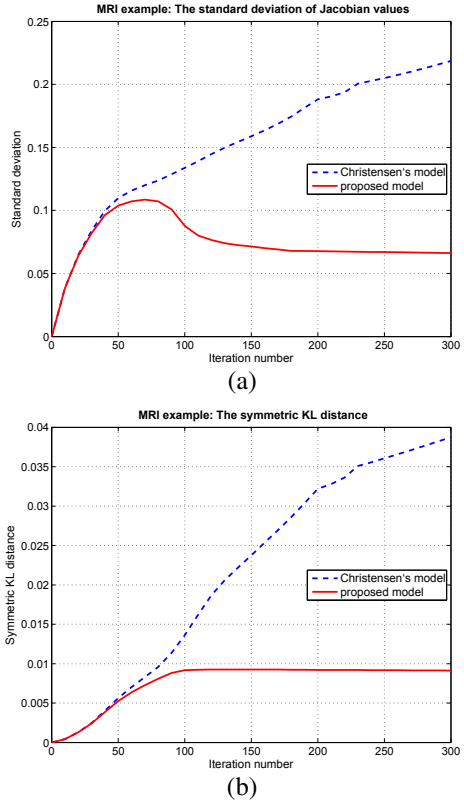

Fig. 5. Serial MRI example. (a) Standard deviation of Jacobian values inside the ventricle per iteration. (b) Symmetric KL distance. For Christensen's model (dashed blue), both standard deviation and symmetric KL distance increase while for the proposed model (solid red), both standard deviation and symmetric KL distance stabilize.

where Co_{ij} is the matrix cofactor of the (i,j)-th component of the Jacobian matrix $D\vec{h}$.

In this paper, we follow the approach in [4] solving the viscous fluid model [5]. Given the velocity field $\vec{v}$, the following partial differential equation can be solved to obtain the displacement field $\vec{u}$: $\partial\vec{u}/\partial t = \vec{v} - \vec{v}\cdot\vec{\nabla}\vec{u}$. The instantaneous velocity as in [4] is obtained by convolving $\vec{f}$ with Gaussian kernel G_σ of variance σ: $\vec{v} = G_\sigma * (-\vec{f}(\vec{x},\vec{u}))$.

3. RESULTS AND DISCUSSION

In this section, we implemented and tested the proposed nonlinear registration model. The deformation fields were computed using adaptive time stepping, with maximal change in displacement of 0.1 allowed in each iteration. In order to obtain a fair comparison between the proposed and the viscous fluid method, re-gridding was not employed. Re-gridding is essentially a memoryless procedure, as how images are matched after each re-gridding is independent of the deformation before the re-gridding, rendering the comparison of final Jacobian fields and cost functionals problematic. Moreover, the strategy of re-gridding, through the relaxation of deformation over time, is less rigorous from a theoretical standpoint.

In Figures 1 through 5, we show the results of matching a pair of 2D slices from a set of Serial MRI images (each of size 226 by 256; $\lambda = 400$ in (4)), where visually significant ventricle enlargement is present. Both the fluid registration (Christensen's) method and the proposed model generated a close match between the deformed image and the study (Figure 1(a-d)). Here, optimal matching was considered achieved once the overall cost functional stopped decreasing. However, as seen in Figures 3 and 4, the proposed method yields intuitively correct results, more evenly distributing deformation inside ventricles (resulting from the convex property of the logarithmic mapping). Notice that in Figure 3, Christensen's method generated a density map with extreme values along the ventricular boundary. Indeed, given the overall longitudinal ventricular dilation, we argue that the corresponding density change map should be constant inside the ventricle. Figure 5(a) plots the standard deviation of the Jacobian field inside the ventricle as a function of iteration number. For Christensen's model, the standard deviation inside the ventricle increased with the number of iterations,while the proposed method yielded an optimized standard deviation as more iterations were computed. The proposed symmetric KL distance also increased for Christensen's method, while it was minimized for the proposed method as shown in Figure 5(b).

In the second numerical example (Figures 6 through 8), we tested the proposed model using two 3D Serial MRI volumes obtained from a patient with right-side temporal atrophy (6 years apart; each of size 112x128x128; $\lambda = 500$). In this example, the same conclusions were reached, demonstrating both the numerical and theoretical advantages of our method. In particular, in Figure 7(b), right temporal atrophy (RT) and ventricular enlargement (V) are easily visualized in the Jacobian map generated using the proposed method, while Christensen's method generated a very noisy map (Figure 7(a)).

4. REFERENCES

[1] B. Avants and J. C. Gee, "Geodesic estimation for large deformation anatomical shape averaging and interpola-

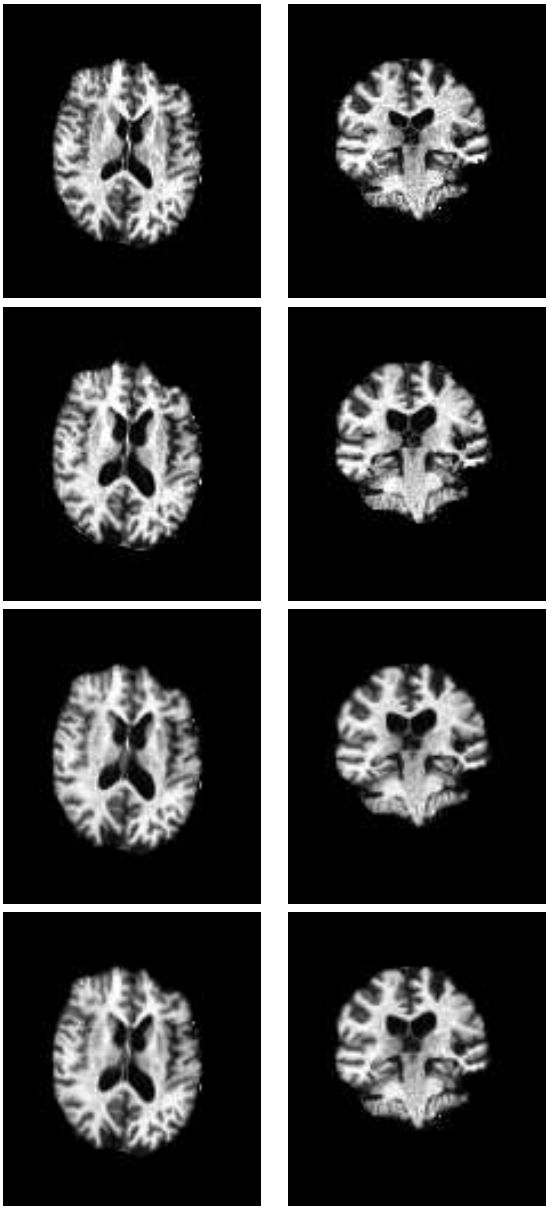

Fig. 6. 3D Serial MRI example. Slices in axial and coronal planes for: T (first row), S (second row), T deformed using Christensen's model (third row), T deformed using the proposed model (fourth row).

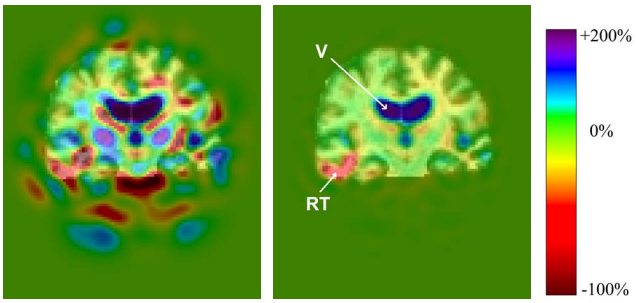

(a) (b)

Fig. 7. 3D Serial MRI example. Jacobian map overlaid with the deformed volume for (a) Christensen's model and (b) the proposed model, with localized atrophy in right temporal area.

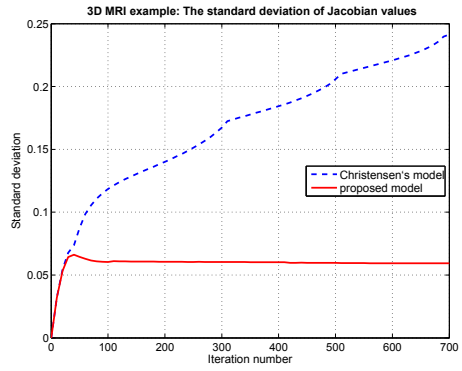

(a)

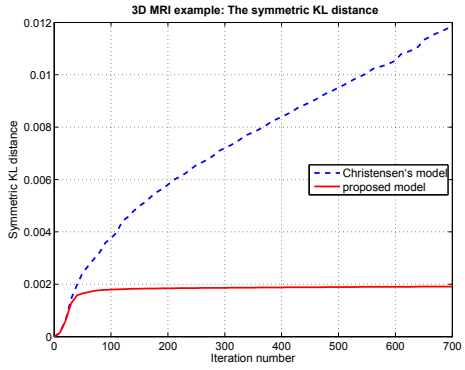

(b)

Fig. 8. 3D Serial MRI example. (a) Standard deviation of Jacobian values inside the ventricle per iteration. (b) Symmetric KL distance.

tion," *NeuroImage*, vol. 23, suppl. 1, S139-50, 2004.

[2] U. Grenander and M. I. Miller, "Computational anatomy: An emerging discipline," *Quarterly of Applied Mathematics*, vol. 56, pp. 617–694, 1998.

[3] P. M. Thompson and A. W. Toga, "A framework for computational anatomy," *Computing and Visualization in Science*, vol. 5, pp. 13–34, 2002.

[4] E. D'Agostino, F. Maes, D. Vandermeulen, and P. Suetens, "A viscous fluid model for multimodal non-rigid image registration using mutual information," *Medical Image Analysis*, vol. 7, pp. 565–575, 2003.

[5] G. Christensen, R. Rabbitt, and M. Miller, "Deformable templates using large deformation kinematics," *IEEE Transactions on Image Processing*, vol. 5, no. 10, pp. 1435–1447, 1996.